Intraoperative ^{68}Ga-PSMA Cerenkov Luminescence Imaging for Surgical Margins in Radical Prostatectomy: A Feasibility Study

Christopher Darr*[1], Nina N. Harke*[1], Jan Philipp Radtke[1], Leubet Yirga[1], Claudia Kesch[1], Maarten R. Grootendorst[2], Wolfgang P. Fendler[3], Pedro Fragoso Costa[3], Christoph Rischpler[3], Christine Praus[3], Johannes Haubold[4], Henning Reis[5], Thomas Hager[5], Ken Herrmann[3], Ina Binse*†[3], and Boris Hadaschik*[1]

[1]*Department of Urology, University Hospital Essen, Essen, Germany;* [2]*Clinical Research, Lightpoint Medical Ltd., Chesham, United Kingdom;* [3]*Department of Nuclear Medicine, University Hospital Essen, Essen, Germany;* [4]*Institute of Diagnostics and Radiology, University Hospital Essen, Essen, Germany;* [5]*Institute of Pathology, University Duisburg–Essen, Essen, Germany; and* [6]*German Cancer Consortium (DKTK), University Hospital Essen, Essen, Germany*

See an invited perspective on this article on page 1498.

Our objective was to assess the feasibility and accuracy of Cerenkov luminescence imaging (CLI) for assessment of surgical margins intraoperatively during radical prostatectomy. **Methods:** A single-center feasibility study included 10 patients with high-risk primary prostate cancer (PC). ^{68}Ga-prostate-specific membrane antigen (PSMA) PET/CT scans were performed followed by radical prostatectomy and intraoperative CLI of the excised prostate. In addition to imaging the intact prostate, in the first 2 patients the prostate gland was incised and imaged with CLI to visualize the primary tumor. We compared the tumor margin status on CLI to postoperative histopathology. Measured CLI intensities were determined as tumor-to-background ratio. **Results:** Tumor cells were successfully detected on the incised prostate CLI images as confirmed by histopathology. Three of 10 men had histopathologically positive surgical margins (PSMs), and 2 of 3 PSMs were accurately detected on CLI. Overall, 25 (72%) of 35 regions of interest proved to visualize a tumor signal according to standard histopathology. The median tumor radiance in these areas was 11,301 photons/s/cm^2/sr (range, 3,328–25,428 photons/s/cm^2/sr), and median tumor-to-background ratio was 4.2 (range, 2.1–11.6). False-positive signals were seen mainly at the prostate base, with PC cells overlaid by benign tissue. PSMA immunohistochemistry revealed strong PSMA staining of benign gland tissue, which impacts measured activities. **Conclusion:** This feasibility showed that ^{68}Ga-PSMA CLI is a new intraoperative imaging technique capable of imaging the entire specimen's surface to detect PC tissue at the resection margin. Further optimization of the CLI protocol, or the use of lower-energy imaging tracers such as ^{18}F-PSMA, is required to reduce false-positives. A larger study will be performed to assess diagnostic performance.

Key Words: Cerenkov luminescence imaging; radioguided surgery; prostate cancer; margin assessment; radical prostatectomy

J Nucl Med 2020; 61:1500–1506
DOI: 10.2967/jnumed.119.240424

Radical prostatectomy (RPE) is one of the primary treatment options for men with localized prostate cancer (PC). The aim of the procedure is complete resection of the prostate without positive surgical margins (PSMs) (*1*). The pentafecta outcome criteria for RPE include continence, potency, lack of early complications, lack of biochemical recurrence, and lack of PSMs and should be fulfilled whenever oncologically possible (*2*).

Incomplete removal of the cancer tissue during RPE may be associated with poorer patient outcomes (*3*). A PSM increases the need for adjuvant radiotherapy, the likelihood of recurrence, and the chances of PC-related mortality by a factor of 3 (*3*). PSMs of more than 3 mm are known to increase the risk of biochemical recurrence (*4*). Similarly, men with persistently elevated PSA levels of at least 0.1 ng/mL more than 6 wk after RPE show less favorable cancer control and survival rates over time (*5–7*).

Next to preoperative MRI for local staging of disease, and nomograms for the prediction of extracapsular extension, the use of intraoperative frozen-section analysis can facilitate the surgeon's decision concerning preservation of functional structures such as the neurovascular bundles (*1,8–10*).

Schlomm et al. described significantly less frequent PSMs of 15% versus 22% for all stages and 21% versus 32% for extraprostatic disease, suggesting that systematic application of intraoperative frozen-section analysis has the potential to significantly increase nerve sparing and to reduce PSMs in RPE (*8*). Other studies, however, demonstrated a high false-negative rate of intraoperative frozen-section analysis, potentially resulting in unjustified nerve-sparing surgery, and eminent time consumption (*11*). Consequently, there is a wish to be able to accurately detect malignant areas in real time during RPE to ensure that the PC is completely removed. Molecular imaging with modern radiopharmaceuticals that target the prostate-specific membrane antigen

Received Dec. 4, 2019; revision accepted Feb. 5, 2020.
For correspondence or reprints contact: Christopher Darr, Department of Urology, University hospital Essen, Hufelandstrasse 55, 45147 Essen, Germany.
E-mail: christopher.darr@uk-essen.de
*Contributed equally to this work.
†Deceased.
Published online Feb. 14, 2020.

(PSMA) can be used for highly specific and sensitive oncologic diagnostic imaging, including initial staging of PC (*12–15*). PSMA PET is an imaging technique that targets PSMA on PC cells, mostly with ^{68}Ga-labeled and ^{18}F-labeled PET agents (*16*).

In recent trials, PSMA PET demonstrated high detection rates for lymph nodes metastases and a positive predictive value for initial staging of PC (*17–20*). Maurer et al. described the advantage of PSMA-radioguided surgery for pelvic lymph node dissection, visualizing even small lymph node metastasis (*21*).

PET imaging agents also emit optical photons via a phenomenon called Cerenkov luminescence, enabling optical molecular imaging in the form of Cerenkov luminescence imaging (CLI) (*22*). CLI and PET are directly correlated, as both techniques measure photons: PET measures the γ-annihilation photons, and CLI measures the Cerenkov photons (*23*). Cerenkov photons are emitted by a charged particle (positron or electron) when traveling through a dielectric medium at a faster speed than the velocity of light in that medium. Although Cerenkov luminescence has a broadband wavelength spectrum, it comprises predominantly ultraviolet and blue light, and as these short wavelengths are highly attenuated in biologic tissue, CLI is limited to detection of signals emitted in superficial tissue layers (~3 mm). In contrast to PET, CLI is unable to detect photons emitted by more deeply located tissues or tumors (*24,25*).

The clinical feasibility and safety of CLI were demonstrated in a small number of breast cancer patients using ^{18}F-FDG (*24*). In that study, good agreement between CLI and histopathology was found for margin distance and invasive cancer tumor size.

To our knowledge, there are no published data available, to date, regarding CLI in PC using a PSMA-labeled tracer. Therefore, the aim of our prospective study was to analyze the feasibility and diagnostic accuracy of intraoperative CLI to detect PSMs in a cohort of 10 men undergoing RPE.

MATERIALS AND METHODS

Patient Recruitment and Patient Preparation on Day of Surgery

Between February 2018 and June 2019, patients with histologically confirmed PC on systematic or MRI-targeted prostate biopsy were recruited at University Hospital Essen after discussion by the local multidisciplinary tumor board and procurement of written informed consent. This study received formal Ethical Committee approval (19-8749-BO). Exclusion criteria were previous prostate surgery or radiotherapy, known distant metastases, and contraindications to surgery.

On the day of surgery, ^{68}Ga-PSMA-11 (1.8–2.2 MBq/kg of body weight) was injected intravenously in patients scheduled to undergo RPE (*26*). At 45–60 min after injection, the PET/CT scan was performed and assessed by experienced nuclear medicine physicians. If any cases of high-volume metastatic disease had been discovered on PET/CT, same-day surgery would have been cancelled.

RPE and Intraoperative CLI

After PET/CT, RPE of these patients was performed by 2 surgeons ahead of extended pelvic lymph node dissection to minimize any reduction in signal intensity from radiotracer decay during ^{68}Ga-PSMA injection and CLI. An indwelling catheter was immediately inserted in the operating theater before surgery to drain the urine and minimize urinary contamination of the prostate. After excision of the prostate, the specimen was immediately retrieved from the abdomen, wiped to clear blood and fluids, positioned in a specimen tray, and imaged in the LightPath CLI system (Lightpoint Medical Ltd.). The LightPath system captured both a Cerenkov image and a photographic image of the specimen in a lighttight imaging chamber and was positioned in the operating room to enable real-time image analysis by the surgeon. Images were acquired with a total time of 300 s and 8×8 pixel binning (*27*). The prostate gland was imaged in different positions, and a total of 2 or 3 images was necessary to capture all sides of the prostate. After the intact prostate was imaged, the prostate gland was incised in the first 2 patients at the level of the main primary lesion as seen on MRI and was subsequently

TABLE 1
Patient and Oncologic Characteristics

Patient no.	Age at surgery (y)	ISUP-GG at PBx	PSA (ng/mL)	BMI (kg/m^2)	T-category	N-category	R-status	Location of PSM/ comment on histopathology	ISUP-GG	ISUP-GG at R1
1	76	5	10.6	24.2	pT3b	pN1	R1	Dorsal, right base (2 mm)	4	5
2	71	4	3.3	25.9	pT3a	pN0	R0	NA	5	NA
3	75	5	14.1	30.1	pT3b	pN1	R0	NA	5	NA
4	76	3	6.9	23.4	pT2a	pN0	R0	NA	3	NA
5	66	4	77.7	30.6	pT3a	pN1	R1	Left apical lobe (8 mm)	5	4
6	63	4	5.3	35.9	pT2c	pN0	R1	Dorsal, right lobe (3 mm)	3	1
7	81	4	11.4	27.1	pT3a	pN0	R0	NA	3	NA
8	72	3	7.1	31.6	pT3a	pN0	R0	NA	2	NA
9	63	5	20	32.1	pT3b	pN1	R0	NA	5	NA
10	68	5	7.48	26.9	pT3a	pN0	R0	NA	2	NA

PBx = prostate biopsy; PSA = prostate specific antigen; BMI = body mass index; gray filled fields = not applicable.

TABLE 2
Overview of Injected Activity and Duration Between Injection, Surgery, and CLI per Patient

Patient no.	Tracer activity at injection (MBq)	Duration until surgery (min)	Duration until CLI (min)	Maximum tracer activity concentration at CLI (kBq/mL)*
1	202	193	313	2.37
2	95	229	340	0.42
3	108	285	429	0.14
4	150	153	285	3.07
5	163	217	282	2.80
6	118	192	304	0.40
7	103	199	326	0.81
8	97	292	391	0.13
9	121	325	420	0.18
10	157	328	409	0.16

*Based on preoperative ^{68}Ga-PSMA PET/CT decay-corrected to time of CLI.

imaged with CLI to visualize the primary tumor. On CLI completion, the prostatectomy specimen was sent for postoperative histopathologic analysis. Because of the design of this feasibility study, the surgical course remained unaffected by the CLI results, and no further tissue was resected if positive margins were suspected on CLI.

Radiation Safety

After completion of CLI, radiation safety was monitored by accurately quantifying the activity in the excised prostate specimen using a high-purity germanium detector (Canberra). The activity was decay-corrected to the time of excision.

Image Analysis

The Cerenkov luminescence images were analyzed postoperatively in a controlled and standardized analysis environment using PMOD (version 3.204; PMOD Technologies). The mean radiance (photons/s/cm^2/sr) was measured by drawing regions of interest (ROIs) on the Cerenkov luminescence images. ROIs were selected in areas showing increased signal intensity (tumor) and no increased signal (tissue background), and tumor-to-background ratios (TBRs) were calculated. Tumor margin assessment on CLI was performed by analyzing elevated signals at the surface of the intact prostate images.

Histopathology and Immunohistochemistry

Histopathologic evaluation was performed adherent to the current German S3-guidelines for PC (*28*). RPEs were evaluated by expert uropathologists, and typical PC metrics were reported, including Gleason grading in its 2014 revision (*29*). PSMA immunohistochemistry was performed on an automated Ventana Benchmark Ultra device (Ventana Medical Systems) using PSMA antibody clone 3E6 (Agilent/DAKO) with a 1:50 dilution. Membranous PSMA expression in immunohistochemistry analyses was stratified according to its primary intensity of staining. Moderate and strong intensities were considered positive (*30*).

RESULTS

In total, 10 patients were included in the presented feasibility study. Their characteristics are displayed in Table 1. Median age at surgery was 72 y, median PSA was 9.04 ng/mL, and median body mass index was 28.6. The median administered ^{68}Ga-PSMA activity was 119 MBq (range, 95–202 MBq). The median time between intravenous injection and the start of surgery was 223 min (range, 153–328 min), and the median time between tracer injection and the beginning of CLI acquisition was 333 min (range, 282–429 min). The median decay-corrected tracer activity at CLI of the prostate was 0.34 kBq/mL (range, 0.13–3.1 kBq/mL; Table 2).

The incised-prostate images acquired for the first 2 patients showed an elevated signal in the primary lesion as confirmed by histopathology (patient 1, TBR of 2.95; patient 2, TBRs of 4.89 for lesion 1 and 4.26 for lesion 2) (Fig. 1).

In total, 23 CLI images of the intact prostate were acquired and analyzed in the 10 patients.

Patients 1, 5, and 6 had a PSM on histopathology (Table 1). In patients 1 and 5, the elevated signal levels enabled correct identification of these margins on CLI (Table 3; Fig. 2). International Society of Urological Pathology Gleason grades (ISUP-GGs) at the resection margin were 5 in patient 1, with a diameter of 2 mm, and 4 in patient 5, with a diameter of 8 mm. Tumor

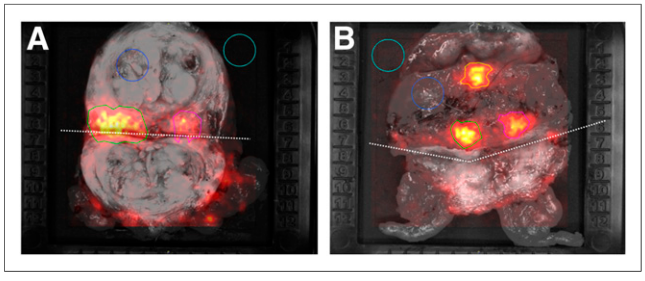

FIGURE 1. Gray-scale photographs overlaid with Cerenkov signals for incised prostate gland specimen of patients 1 (A) and 2 (B). In each image, ROIs are encircled. Incision is marked with dotted line. Light blue ROI (area of empty specimen tray) and dark blue ROI (area of normal prostate tissue) were used as empty background and tissue background, respectively. Green ROI (lesion 1) and pink ROI (lesion 2) show increased signal; histopathologic analysis confirmed cancer tissue in these areas. Orange ROI in B shows increased signal from area without cancer cells.

TABLE 3
CLI Measurements

Patient no.	Placement	Prostate tissue background	ROI 1		ROI 2		ROI 3		ROI 4	
			Measurements	Location	Measurements	Location	Measurements	Location	Measurements	Location
1	Base down	1,895 (±343)	6,101 (±743)*; TBR: 3.22*	Dorsal, left base*	7,376 (±1,628); TBR: 3.89	Right ventral apex	NA	NA	NA	NA
	Posterior down	2,845 (±357)	12,409 (±4,040)*; TBR: 4.36*	Whole base*	7900 (±1,461); TBR: 2.78	Ventral central	19,061 (±3,689)*†; TBR: 6.7*†	Right base*†	NA	NA
	Posterior down (incised base)	2,192 (±319)	6,468 (±1,207)*; TBR: 2.95*	Left base incised*	5,400 (±745); TBR: 2.46	Right base incised	NA	NA	NA	NA
2	Ventral down	1,507 (±209)	5,106 (±1,482)*; TBR: 3.39*	Right base*	NA	NA	NA	NA	NA	NA
	Posterior down	2,426 (±285)	11,383 (±5,591)*; TBR: 4.69*	Whole base*	9,802 (±1,922); TBR: 4.04	Ventral central	19,399 (±3,079)*; TBR: 8.0*	Right base*	22,350 (±4,464)*; TBR: 9.21*	Left base*
	Posterior down (incised base)	2,155 (±353)	10,538 (±2,567)*; TBR: 4.89*	Left base incised*	9,188 (±1,752)*; TBR: 4.26*	Right base incised*	10,239 (±2,378); TBR: 4.75	Ventral central	NA	NA
3	Posterior down	1,695 (±333)	5,035 (±1,008); TBR: 2.97	Left base	NA	NA	NA	NA	NA	NA
	Base down	1,949 (±345)	NA	NA	NA	NA	NA	NA	NA	NA
4	Posterior down	2,001 (±275)	8,069 (±2,676)*; TBR: 4.03*	Central base*	6,031 (±1,285); TBR: 3.01	Ventral apex	NA	NA	NA	NA
	Base down	1,651 (±287)	3,526 (±877)*; TBR: 2.14*	Dorsal, left base*	5,376 (±1,265); TBR: 3.26	Ventral apex	NA	NA	NA	NA
5	Apex down	5,310 (±1,447)	18,664 (±5,258)*; TBR: 3.51*	Central base*	25,428 (±4,351)*; TBR: 4.79*	Left base*	NA	NA	NA	NA
	Posterior down	3,219 (±504)	6,131 (±1,686)*†; TBR: 1.9*†	Left ventral apex*†	6,242 (±1,984)*†; TBR: 1.94*†	Right and left base*†	NA	NA	NA	NA
	Ventral down	1,663 (±231)	3,328 (±535)*; TBR: 2.0*	Dorsal base left > right*	NA	NA	NA	NA	NA	NA
6	Apex down	1,967 (±293)	9,964 (±2,718); TBR: 5.07	Right base	5,146 (±2,378); TBR: 2.62	Central base	NA	NA	NA	NA
	Posterior down	1,650 (±256)	3,436 (±793)*; TBR: 2.08*	Apex ventral*	NA	NA	NA	NA	NA	NA
7	Base down	2,559 (±520)	8,888 (±1,867)*; TBR: 3.47*	Apex ventral*	NA	NA	NA	NA	NA	NA
	Posterior down	2,390 (±533)	28,048 (±5,403)*; TBR: 11.59*	Right base*	6,846 (±2,178); TBR: 5.86	Left base	NA	NA	NA	NA
8	Posterior down	2,847 (±514)	18,565 (±4,056)*; TBR: 6.52*	Right base*	20,282 (±2,979)*; TBR: 7.12*	Left base*	NA	NA	NA	NA
	Base down	1,739 (±260)			NA	NA	NA	NA	NA	NA
	Ventral down	1,715 (±288)			NA	NA	NA	NA	NA	NA
9	Posterior down	3,105 (±444)	13,039 (±3,850)*; TBR: 4.20*	Left base*	11,716 (±2,991)*; TBR: 3.77*	Central base*	NA	NA	NA	NA
	Base down	2,528 (±364)			NA	NA	NA	NA	NA	NA
10	Ventral down	1,742 (±295)			NA	NA	NA	NA	NA	NA
	Base down	1,832 (±278)	4,205 (±1,023)*; TBR: 2.3*	Apex ventral*	NA	NA	NA	NA	NA	NA
	Posterior Down	2,662 (±407)	24,520 (±6,428)*; TBR: 9.21*	Right base*	23,969 (±5,235)*; TBR: 9.0*	Left base*	11,218 (±4,251)*; TBR: 4.21*	Ventral apex*	NA	NA

*Elevated Cerenkov luminescence activity with histopathologic proof of PC tissue (<3 mm).
†Region in which histopathologically positive resection margins were detected.
NA = not applicable.
Activity levels are mean ± SD photons/s/cm^2/sr.

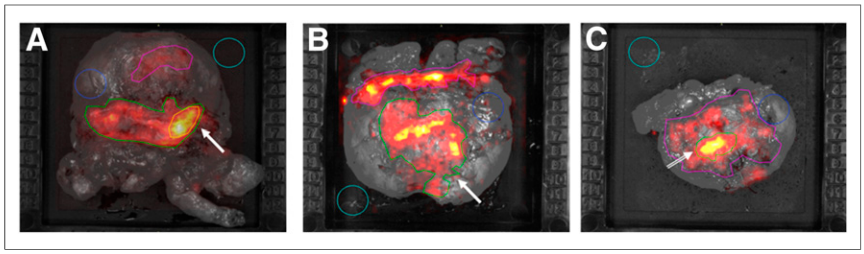

FIGURE 2. Gray-scale photographs overlaid with Cerenkov signal for patients 1 (A), 5 (B), and 6 (C), with PSMs. Elevated signal (arrow) from tumor can be seen in A and B. Elevated signal without histopathologic tumor cell correlation is displayed in C (arrow). Immunohistochemistry showed PSMA expression of benign tissue in this region.

radiance and TBR were 19,061 and 6.7, respectively, in patient 1 and 6,131 and 1.9, respectively, in patient 5. In patient 6, no elevated signal could be identified on CLI, and this patient had an ISUP-GG of 1 at the margin (right dorsal lobe) on histopathology, with a diameter of 3 mm.

In total, 35 ROIs were drawn in areas displaying an elevated CLI signal: 24 in the base, 8 in the apex, and 3 in the ventral side (Table 3). However, 25 of the 35 ROIs (71.5%) were confirmed by pathology to contain tumor cells, some with margins of up to 3 mm. The median tumor radiance in these areas was 11,301 photons/s/cm^2/sr (range, 3,328–25,428 photons/s/cm^2/sr), and the median TBR was 4.2 (range, 2.1–11.6).

PSMA immunohistochemistry was performed on the last slices of the prostate base in the first 8 patients for whom standard histopathology suggested false-positive results, to assess PSMA expression in these areas (Fig. 3; Table 4). PSMA immunohistochemistry demonstrated a moderate to strong PSMA immunohistochemistry signal that corresponded to CLI in benign tissue in 7 of 8 patients. In 5 (62.5%) patients, underlying PC tissue with PSMA immunohistochemistry expression was also observed. All cancer areas showed an elevated CLI intensity.

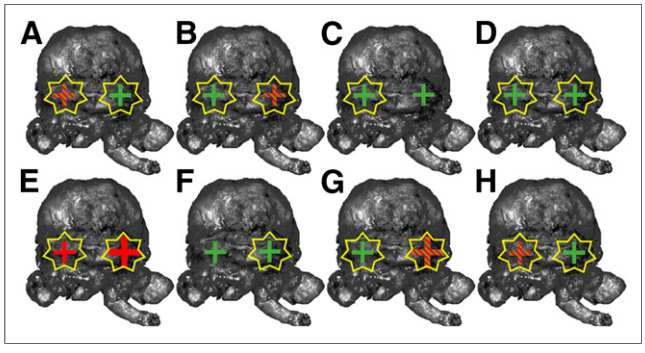

FIGURE 3. PSMA immunohistochemistry correlation of prostate base, running from patient 1 (A) to patient 8 (H). Green crosses = PSMA immunohistochemistry expression of benign gland tissue; red crosses = PSMA immunohistochemistry expression of carcinoma; green and red striped crosses = PSMA immunohistochemistry expression of benign gland tissue and carcinoma. Crosses display analyzed side (left or right prostate base). Additionally, larger crosses symbolize higher amount of tumor cells. Yellow stars display increased Cerenkov intensity in this area.

In 4 patients, radiation safety measurements were performed and demonstrated that the intensity level in the excised specimen was below the permitted exemption levels stipulated by the German radiation protection ordinance (^{68}Ga $<$ 100 kBq).

DISCUSSION

This first-in-men study evaluated the feasibility of intraoperative ^{68}Ga-PSMA CLI for assessing tumor margin status in patients with high-risk primary PC undergoing RPE and extended pelvic lymph node dissection. CLI seems to be able to successfully detect positive histopathologic resection margins with high ISUP-GGs, and all ROIs containing PSMA-immunohistochemistry–positive cancer tissue showed elevated Cerenkov intensity. The low ^{68}Ga-PSMA activity at the time of surgery implies that the prostate specimen presents no considerable radiation burden for the CLI operator or pathologist and can be treated as nonradioactive material.

One patient had a PSM with an ISUP-GG of 1, but this margin did not display an increased signal on CLI. As these low-grade cancers are known to have a lower PSMA expression, this finding may explain false-negative CLI results (*30*).

To further examine Cerenkov signals, we incised the prostate gland at the main tumor lesion in 2 patients. In both patients, 2 suggestive areas were detected. Correlation of histopathology and CLI proved a detection rate of 100% in patient 2 and 50% in patient 1. In patient 1, superficial cancer cells were described on the left side. Because the main cancer nidus was at the right dorsal prostate base, we assume that the cancer tissue was overlaid through a thin layer of normal tissue and therefore could be not visualized on CLI. This assumption is supported through the higher TBR of the left ROI (2.95 vs. 2.46).

Although ^{68}Ga-PSMA CLI of prostatectomy specimens seems feasible for assessing the status of tumor-resection margins, 10 of the 35 ROIs showed elevated signal levels without histopathologic evidence of PC tissue at the resection margin. There are several possible reasons for these false-positive findings. First, CLI intensity can emerge from PSMA expression and tracer uptake in noncancerous tissues. To analyze the prostate base, where CLI was positive despite negative histopathology findings, PSMA immunohistochemistry of the last slice of the prostate base was performed on 8 patients. In 14 of 16 (87%) areas, PSMA staining of benign tissue was observed. Eight of these may have caused a false-positive signal on CLI because they were close to the tissue's surface. Second, the mean positron range of ^{68}Ga is ±2.8 mm (*31*), and thus, Cerenkov luminescence can be produced from a few millimeters underneath the tissue's surface. To enable more superficial imaging, a short-pass optical filter might be used in the future to exclude the longer-wavelength Cerenkov photons that have a deeper tissue penetration (i.e., the red and near-infrared Cerenkov photons). Another option would be to use an ^{18}F-labeled PSMA tracer such as ^{18}F-PSMA-1007 (*17*). As ^{18}F positrons have a lower energy than ^{68}Ga (0.64 vs. 1.9 MeV), the mean positron range in tissue is significantly shorter (0.54 vs. 2.83 mm), thus

TABLE 4
PSMA Immunohistochemistry

Patient no.	Anatomic region	PSMA immunohistochemistry expression	
		Carcinoma	Benign
1	Right lobe, prostate base	Negative	Positive
	Left lobe, prostate base	Positive	Positive
	Transition to left seminal vesicle	Positive	Positive
	Transition to right seminal vesicle	Negative	Positive
2	Right lobe, prostate base	Positive	Positive
	Transition to right seminal vesicle	Negative	Positive
	Transition to left seminal vesicle	Negative	Positive
3	Right bladder neck	Negative	Positive
	Left bladder neck	Negative	Positive
4	Right lobe, prostate base	Negative	Positive
	Left lobe, prostate base	Negative	Positive
	Right bladder neck	Negative	Positive
	Left bladder neck	Negative	Positive
5	Transition to right seminal vesicle	Positive	Negative
	Transition to left seminal vesicle	Positive	Negative
6	Right lobe, prostate base	Negative	Positive
	Left lobe, prostate base	Negative	Positive
7	Transition to right seminal vesicle	Positive	Positive
	Transition to left seminal vesicle	Negative	Positive
	Right bladder neck	Negative	Positive
	Left bladder neck	Negative	Positive
8	Right lobe, prostate base	Negative	Positive
	Left lobe, prostate base	Positive	Positive
	Transition to left seminal vesicle	Positive	Positive
	Transition to right seminal vesicle	Negative	Positive

For further analysis of prostate base, selective staining of last slices of prostate base was performed. Positive result indicated moderate to strong PSMA expression.

facilitating submillimeter margin assessment (*31*). Lastly, ^{68}Ga-PSMA-11 is known to be excreted via the urinary tract, thus potentially causing elevated signals at the bladder neck or prostate base through urinary contamination (*32*). One method for minimizing the risk of prostate surface contamination from urine is to rinse the prostate with sodium chloride solution before CLI image acquisition. However, this step was not performed in this study. Another method would be to use a tracer that has nonrenal clearance, such as ^{18}F-PSMA-1007 (*17,33*).

The preclinical study by Olde Heuvel et al. found 0.14 kBq/mL to be the minimum detectable intensity for a 300-s 8 × 8 binning acquisition (*34*). Because of the long interval between tracer injection and CLI in our study (~6 h), the activity levels in the prostate at the time of CLI were low (median ^{68}Ga-PSMA activity of 0.34 kBq/mL) and close to the limit of detection. To avoid a loss of imaging quality, a long acquisition time is essential. Nevertheless, tumor margin assessment on CLI could be performed in all 10 patients. To increase the difference in CLI signal intensity between benign and PC tissue, the time from injection to CLI can be reduced. Such a reduction may improve the detectability of PSMA cancers of low avidity, including low ISUP-GG. Alternatively, the workflow could be changed so that on the day of surgery no PET imaging is performed and only a reduced amount of tracer is injected.

Long-term prediction of PC-specific mortality is based mainly on histopathology features as described by Eggener et al.: poorly differentiated cancer, with a Gleason grade of 8–10, and seminal vesicle invasion are prime determinants of PC-specific mortality after RPE (*35*). Findings of Martini et al. demonstrated that only unfavorable PSMs (≥3 mm or multifocal positive margins) significantly influence the risk of metastasis in PC (*36*). Currently, intraoperative frozen-section analysis is the gold standard for assessing removal of all PC tissue. If the addition of short-pass optical filters reduces the penetration depth of CLI, frozen-section analysis might, in the future, be reduced to conspicuous areas only.

To assess sensitivity and specificity, a single-center clinical study is scheduled to commence in early 2020. The recruitment target is 40 patients, with the first patient expected to be recruited in quarter 1 of 2020. In these patients, the CLI protocol will be improved by implementing a short-pass optical filter. In parallel to the planned clinical study, we are performing preclinical experiments using 3-dimensionally printed prostate models to evaluate the penetration depth and resolution of CLI in correlation with tracer activity levels.

CLI uses nuclear medicine methods to inform urologic surgery for improved local treatment of PC. This new imaging modality brings the urology and nuclear medicine communities more closely together in making progress on PC (*37*).

CONCLUSION

Intraoperative ^{68}Ga-PSMA CLI in PC is a promising tool to improve surgery. CLI provides high-resolution information on the whole prostate gland that may assist surgeons in assessing margin status by providing a good correlation to histopathologic examination.

DISCLOSURE

Maarten Grootendorst in an employee of Lightpoint Medical Ltd. Wolfgang P. Fendler is a consultant for Ipsen, Endocyte, and BTG and received personal fees from RadioMedix outside the submitted work. No other potential conflict of interest relevant to this article was reported.

KEY POINTS

QUESTION: Is CLI useful for displaying PC cells near or at the surface of the prostatectomy specimen?

PERTINENT FINDINGS: In this feasibility study of 10 patients undergoing radical prostatectomy with a ^{68}Ga-PET/CT scan on the same day, CLI was able to detect cancer cells near and at the surface of the prostate. These results are the basis for initiation of further prospective studies.

IMPLICATIONS FOR PATIENT CARE: CLI is a promising technique for intraoperative evaluation of the whole prostate surface regarding PSMs.

REFERENCES

1. EAU guidelines on upper urinary tract urothelial carcinoma. Arnhem, The Netherlands: EAU Guidelines Office; 2019. https://uroweb.org/wp-content/uploads/EAU-Guidelines-on-Upper-urinary-Tract-Tumours-2019.pdf. Accessed September 4, 2020.
2. Patel VR, Sivaraman A, Coelho RF, et al. Pentafecta: a new concept for reporting outcomes of robot-assisted laparoscopic radical prostatectomy. *Eur Urol.* 2011;59:702–707.
3. Wright JL, Dalkin BL, True LD, et al. Positive surgical margins at radical prostatectomy predict prostate cancer specific mortality. *J Urol.* 2010;183:2213–2218.
4. Kozal S, Peyronnet B, Cattarino S, et al. Influence of pathological factors on oncological outcomes after robot-assisted radical prostatectomy for localized prostate cancer: results of a prospective study. *Urol Oncol.* 2015;33:330.e1–330.e7.
5. Rogers CG, Khan MA, Craig Miller M, Veltri RW, Partin AW. Natural history of disease progression in patients who fail to achieve an undetectable prostate-specific antigen level after undergoing radical prostatectomy. *Cancer.* 2004;101:2549–2556.
6. Bianchi L, Nini A, Bianchi M, et al. The role of prostate-specific antigen persistence after radical prostatectomy for the prediction of clinical progression and cancer-specific mortality in node-positive prostate cancer patients. *Eur Urol.* 2016;69:1142–1148.
7. Preisser F, Chun FKH, Pompe RS, et al. Persistent prostate-specific antigen after radical prostatectomy and its impact on oncologic outcomes. *Eur Urol.* 2019;76:106–114.
8. Schlomm T, Tennstedt P, Huxhold C, et al. Neurovascular structure-adjacent frozen-section examination (NeuroSAFE) increases nerve-sparing frequency and reduces positive surgical margins in open and robot-assisted laparoscopic radical prostatectomy: experience after 11,069 consecutive patients. *Eur Urol.* 2012;62:333–340.
9. Nyarangi-Dix J, Wiesenfarth M, Bonekamp D, et al. Combined clinical parameters and multiparametric magnetic resonance imaging for the prediction of extraprostatic disease: a risk model for patient-tailored risk stratification when planning radical prostatectomy. *Eur Urol Focus.* November 23, 2018 [Epub ahead of print].
10. Petralia G, Musi G, Padhani AR, et al. Robot-assisted radical prostatectomy: multiparametric MR imaging-directed intraoperative frozen-section analysis to reduce the rate of positive surgical margins. *Radiology.* 2015;274:434–444.
11. Gillitzer R, Thuroff C, Fandel T, et al. Intraoperative peripheral frozen sections do not significantly affect prognosis after nerve-sparing radical prostatectomy for prostate cancer. *BJU Int.* 2011;107:755–759.
12. Perera M, Papa N, Roberts M, et al. Gallium-68 prostate-specific membrane antigen positron emission tomography in advanced prostate cancer: updated diagnostic utility, sensitivity, specificity, and distribution of prostate-specific membrane antigen-avid lesions—a systematic review and meta-analysis. *Eur Urol.* 2020;77:403–417.
13. Yaxley JW, Raveenthiran S, Nouhaud FX, et al. Risk of metastatic disease on ^{68}gallium-prostate-specific membrane antigen positron emission tomography/computed tomography scan for primary staging of 1253 men at the diagnosis of prostate cancer. *BJU Int.* 2019;124:401–407.
14. Koschel S, Murphy DG, Hofman MS, Wong LM. The role of prostate-specific membrane antigen PET/computed tomography in primary staging of prostate cancer. *Curr Opin Urol.* 2019;29:569–577.
15. Kalapara AA, Nzenza T, Pan HY, et al. Detection and localisation of primary prostate cancer using ^{68}Ga-PSMA PET/CT compared with mpMRI and radical prostatectomy specimens. *BJU Int.* July 1, 2019 [Epub ahead of print].
16. Schwarzenboeck SM, Rauscher I, Bluemel C, et al. PSMA ligands for PET imaging of prostate cancer. *J Nucl Med.* 2017;58:1545–1552.
17. Kesch C, Vinsensia M, Radtke JP, et al. Intraindividual comparison of ^{18}F-PSMA-1007 PET/CT, multiparametric MRI, and radical prostatectomy specimens in patients with primary prostate cancer: a retrospective, proof-of-concept study. *J Nucl Med.* 2017;58:1805–1810.
18. Giesel FL, Hadaschik B, Cardinale J, et al. F-18 labelled PSMA-1007: biodistribution, radiation dosimetry and histopathological validation of tumor lesions in prostate cancer patients. *Eur J Nucl Med Mol Imaging.* 2017;44:678–688.
19. Herlemann A, Wenter V, Kretschmer A, et al. ^{68}Ga-PSMA positron emission tomography/computed tomography provides accurate staging of lymph node regions prior to lymph node dissection in patients with prostate cancer. *Eur Urol.* 2016;70:553–557.
20. van Kalmthout LWM, van Melick HHE, Lavalaye J, et al. Prospective validation of gallium-68 PSMA-PET/CT in primary staging of prostate cancer patients. *J Urol.* 2020;203:537–545.
21. Maurer T, Weirich G, Schottelius M, et al. Prostate-specific membrane antigen-radioguided surgery for metastatic lymph nodes in prostate cancer. *Eur Urol.* 2015;68:530–534.
22. Das S, Thorek DL, Grimm J. Cerenkov imaging. *Adv Cancer Res.* 2014;124:213–234.
23. Grootendorst MR, Cariati M, Kothari A, Tuch DS, Purushotham A. Cerenkov luminescence imaging (CLI) for image-guided cancer surgery. *Clin Transl Imaging.* 2016;4:353–366.
24. Grootendorst MR, Cariati M, Pinder SE, et al. Intraoperative assessment of tumor resection margins in breast-conserving surgery using ^{18}F-FDG Cerenkov luminescence imaging: a first-in-human feasibility study. *J Nucl Med.* 2017;58:891–898.
25. Chin PT, Welling MM, Meskers SC, Valdes Olmos RA, Tanke H, van Leeuwen FW. Optical imaging as an expansion of nuclear medicine: Cerenkov-based luminescence vs fluorescence-based luminescence. *Eur J Nucl Med Mol Imaging.* 2013;40:1283–1291.
26. Fendler WP, Eiber M, Beheshti M, et al. ^{68}Ga-PSMA PET/CT: joint EANM and SNMMI procedure guideline for prostate cancer imaging—version 1.0. *Eur J Nucl Med Mol Imaging.* 2017;44:1014–1024.
27. Ciarrocchi E, Vanhove C, Descamps B, De Lombaerde S, Vandenberghe S, Belcari N. Performance evaluation of the LightPath imaging system for intraoperative Cerenkov luminescence imaging. *Phys Med.* 2018;52:122–128.
28. Interdisziplinäre leitlinie der qualität S3 zur früherkennung, diagnose und therapie der verschiedenen stadien des prostatakarzinoms. AWMF website. https://www.awmf.org/leitlinien/detail/ll/043-022OL.html. Accessed May 4, 2020.
29. Epstein JI, Egevad L, Amin MB, Delahunt B, Srigley JR, Humphrey PA. The 2014 International Society of Urological Pathology (ISUP) consensus conference on Gleason grading of prostatic carcinoma: definition of grading patterns and proposal for a new grading system. *Am J Surg Pathol.* 2016;40:244–252.
30. Hupe MC, Philippi C, Roth D, et al. Expression of prostate-specific membrane antigen (PSMA) on biopsies is an independent risk stratifier of prostate cancer patients at time of initial diagnosis. *Front Oncol.* 2018;8:623.
31. Moses WW. Fundamental limits of spatial resolution in PET. *Nucl Instrum Methods Phys Res A.* 2011;648(suppl 1):S236–S240.
32. Budäus L, Leyh-Bannurah SR, Salomon G, et al. Initial experience of ^{68}Ga-PSMA PET/CT imaging in high-risk prostate cancer patients prior to radical prostatectomy. *Eur Urol.* 2016;69:393–396.
33. Giesel FL, Will L, Kesch C, et al. Biochemical recurrence of prostate cancer: initial results with [^{18}F]PSMA-1007 PET/CT. *J Nucl Med.* 2018;59:632–635.
34. Olde Heuvel J, de Wit-van der Veen BJ, Vyas KN, et al. Performance evaluation of Cerenkov luminescence imaging: a comparison of ^{68}Ga with ^{18}F. *EJNMMI Phys.* 2019;6:17.
35. Eggener SE, Scardino PT, Walsh PC, et al. Predicting 15-year prostate cancer specific mortality after radical prostatectomy. *J Urol.* 2011;185:869–875.
36. Martini A, Gandaglia G, Fossati N, et al. Defining clinically meaningful positive surgical margins in patients undergoing radical prostatectomy for localised prostate cancer. *Eur Urol Oncol.* April 4, 2019 [Epub ahead of print].
37. Murphy DG, Hofman MS, Azad A, Violet J, Hicks RJ, Lawrentschuk N. Going nuclear: it is time to embed the nuclear medicine physician in the prostate cancer multidisciplinary team. *BJU Int.* May 24, 2019 [Epub ahead of print].